Published in final edited form as:
J Biol Chem. 2007 October 19; 282(42): 30452–30465.

Glutathione Depletion Is Necessary for Apoptosis in Lymphoid Cells Independent of Reactive Oxygen Species Formation*

Rodrigo Franco, **Mihalis I. Panayiotidis**[1], and **John A. Cidlowski**[2]
From the Laboratory of Signal Transduction, NIEHS, National Institutes of Health, Research Triangle Park, North Carolina 27709

Abstract

Changes in the intracellular redox environment of cells have been reported to be critical for the activation of apoptotic enzymes and the progression of programmed cell death. Glutathione (GSH) depletion is an early hallmark observed in apoptosis, and we have demonstrated that GSH efflux during death receptor-mediated apoptosis occurs via a GSH transporter. We now evaluate the relationship between GSH depletion, the generation of reactive oxygen species (ROS), and the progression of apoptosis. Simultaneous single cell analysis of changes in GSH content and ROS formation by multiparametric FACS revealed that loss of intracellular GSH was paralleled by the generation of different ROS including hydrogen peroxide, superoxide anion, hydroxyl radical, and lipid peroxides. However, inhibition of ROS formation by a variety of antioxidants showed that GSH loss was independent from the generation of ROS. Furthermore, GSH depletion was observed to be necessary for ROS generation. Interestingly, high extracellular thiol concentration (GSH and *N*-acetyl-cysteine) inhibited apoptosis, whereas, inhibition of ROS generation by antioxidants was ineffective in preventing cell death. Finally, GSH depletion was shown to be a necessary for the progression of apoptosis activated by both extrinsic and intrinsic signaling pathways. These results document a necessary and critical role for GSH loss in apoptosis and clearly uncouple for the first time GSH depletion from ROS formation.

Apoptosis or programmed cell death is a ubiquitous, evolutionary conserved process. Under physiological conditions it is important not only in the turnover of cells in all tissues, but also during the normal development and senescence of the organism. Moreover, its deregulation has been observed to occur as either a cause or consequence of distinct pathologies (1,2). For example, apoptosis mediated by Fas ligand (FasL)[3] receptor (Fas/CD95/Apo-1) activation is necessary for the immune system homeostasis because of its role in the rapid clearance of immunoreactive T cells maintaining the immune balance and reducing the risk of autoimmune diseases (3). Apoptosis is a highly organized process characterized by the progressive activation of precise pathways leading to specific biochemical and morphological alterations. Initial stages of apoptosis are characterized by reactive oxygen species formation, changes in intracellular ionic homeostasis, cell shrinkage, loss of membrane lipid asymmetry, and

*This research was supported by the Intramural Research Program of the NIEHS, National Institutes of Health.

2To whom correspondence should be addressed: Laboratory of Signal Transduction, NIEHS, National Institutes of Health. P. O. Box 12233. 111. T.W. Alexander Drive. Research Triangle Park, NC 27709. Tel.: 919-541-1564; Fax: 919-541-1367; E-mail: cidlows1@mail.nih.gov.
[1]Current address: School of Public Health, University of Nevada at Reno, Reno, NV 89557.

[3]The abbreviations used are: FasL, Fas ligand; GSH, reduced glutathione; OA^-, organic anion; ROS, reactive oxygen species; RNS, reactive nitrogen species; $^{\bullet}O_2^-$, superoxide anion; $^{\bullet}OH$, hydroxyl radical; $^1O_2$, singlet oxygen; NO, nitric oxide; $OONO^-$, peroxynitrite; H_2O_2, hydrogen peroxide; LPO, lipid peroxides; NAC, *N*-acetyl-cysteine; ANT-CK, antioxidant cocktail; PBS, phosphate-buffered saline; FACS, fluorescence-activated cell sorting; FITC, fluorescein isothiocyanate; DIC, differential interference contrast; PARP, poly (ADP-ribose) polymerase; BSO, DL-buthionine-(*S*,*R*)-sulfoximine; DHR, dihydrorhodamine; DHE, dihydroethidium; HPF, 3″-(*p*-hydroxyphenyl) fluorescein; mBCl, monochlorobimane.

chromatin condensation. Later stages associated with the execution phase of apoptosis are characterized by activation of execution caspases and endonucleases, apoptotic body formation, and cell fragmentation (1,4,5).

Apoptosis has been widely reported to be modulated by changes in the redox status of the cell; however, the precise mechanisms involved are still unclear (6,7). Reduced glutathione (GSH) is the most abundant low molecular weight thiol in animal cells and is involved in many cellular processes including antioxidant defense, drug detoxification, cell signaling, and cell proliferation (8,9). In addition, alterations in its concentration have been demonstrated as a common feature of many pathological situations including AIDS, neurodegenerative diseases, and cancer (9,10). Intracellular GSH loss is an early hallmark in the progression of cell death in response to different apoptotic stimuli (11–14), and has been associated with the activation of a plasma membrane transport mechanism rather than to its oxidation (11–13,15–17). Furthermore, several studies have shown a correlation between cellular GSH depletion and the progression of apoptosis (12,13). Additionally, high GSH levels have also been associated with an apoptotic resistant phenotype in different cells (18–21). We have recently shown that Fas ligand (FasL)-induced GSH efflux is mediated by its extrusion across the plasma membrane in lymphoid cells with characteristics of GSH/organic anion transporter (13); however, the mechanisms involved in the regulation of apoptosis by changes in intracellular GSH are not completely understood.

Because of its action as a primary intracellular antioxidant in the cells, a reduction in the intracellular glutathione content has primarily been thought to reflect the generation of reactive species of oxygen (ROS) and nitrogen (RNS) (6,7). Although, the role of ROS in apoptosis has been extensively studied (6,7), contradictory results including both inhibitory and stimulatory effects of ROS on apoptosis have been reported. For example, induction of apoptosis by activation of the Fas receptor has been suggested to be dependent on the generation of H_2O_2 formation (20,22–26), while other studies report an inhibitory role of H_2O_2 on Fas-mediated cell death (27–29).

In the present work, we evaluate the relationship between GSH depletion, ROS generation, and their respective roles in apoptosis at the single cell level. We present evidence that clearly uncouples for the first time the role of GSH depletion in apoptosis from the generation of ROS. Furthermore, we demonstrate that changes in GSH content are necessary for apoptosis to occur. In contrast increases in ROS did not modulate apoptotic cell death. Our data suggest an important role for changes in intracellular GSH content in the activation of programmed cell death independent from increases in ROS formation.

EXPERIMENTAL PROCEDURES

Reagents

RPMI 1640, penicillin/streptomycin, heat-inactivated fetal calf serum, sodium pyruvate and were from Invitrogen. MK571 was purchased from BioMol (Plymouth, PA). *N*-Acetyl-L-cysteine (NAC), deferoxamine mesylate (also known as desferrioxamine or desferroxamine), ebselen, diphenylene-iodonium (DPI), catalase (bovine liver), Mn-TBAP (Mn(III)tetrakis(4-benzoic acid) porphyrin chloride), MnTE-2-PyP (manganese(III)-5,10,15,20-tetrakis(*N*-ethylpyridinium-2-yl) porphyrin pentachloride), and trolox were from Calbiochem/EMD Biosciences Inc. (San Diego, CA). Mono-chlorobimane (mBCl), dihydrorhodamine 123 (DHR), 3″-(*p*-hydroxyphenyl) fluorescein (HPF), dihydroethidium (DHE), 4,4-difluoro-5,7-dimethyl-4-bora-3a,4a-diaza-*s*-inda-cene-3-propio-nyl ethylenediamine hydrochloride (BODIPY® FL EDA), *cis*-parinaric acid (CsPA), DAF-FM, carboxy-PTIO, TOTO-3, and Singlet Oxygen Sensor Green were from Molecular Probes Inc. (Eugene, OR). Cytofix/cytoperm kit, and the monoclonal antibodies FITC-conjugated anti-active caspase 3, and PE-

conjugated anti-poly(ADP-ribose) polymerase (PARP) cleaved site-specific were from BD Biosciences (San Diego, CA). Anti-cleaved caspase 3, anti-caspase-3, anti-caspase-6, anti-caspase-7, anti-PARP, and anti-α-fodrin antibodies were from Cell Signaling Technology Inc (Beverly, MA). All other reagents were from Sigma/Aldrich.

Cell Culture and Media

Jurkat cells, E6.1 clone (human leukemia) were obtained from American Tissue Culture Collection (Manassas, VA). Cells were cultured in RPMI 1640 medium containing 10% heat-inactivated fetal calf serum, 2 mM glutamine, 31 mg/liter penicillin, and 50 mg/liter streptomycin at 37 °C, 7% CO_2 atmosphere. Apoptosis was induced by incubating cells (5–7 × 10^5 cells/ml) at 37 °C, 7% CO_2 for the time indicated with either human recombinant FasL (Kamiya Biomedical Co.), cycloheximide, etoposide or treatment with ultraviolet C light (UVC) light in a UV Stratalinker 1800 (Stratagene). In media containing high GSH (+GSH) or NAC (+NAC), NaCl was substituted with 25 mM L-glutathione or 10 mM NAC, maintaining the same osmolarity of the media. Media osmolarity was measured on a Wescor 5500 vapor pressure osmometer (Logan, UT).

Fluorescence-activated Cell Sorting (FACS)

Apoptotic parameters were analyzed by FACS, using a BD LSR II flow cytometer and BD FACSDiva Software (Becton Dickinson, San Jose, CA) for data analysis. Samples were analyzed and in all cases 1 × 10^4 cells were recorded. Fluorophores were diluted in Me_2SO or dimethylformamide (DMF) and preloaded just prior to FACS analysis and incubated at 37 °C, 7% CO_2 in cell culture medium, unless otherwise indicated. Control cells were incubated with vehicles, which never exceed 0.1% in the final concentration. Propidium iodide (PI) was added to a final concentration of 10 μg/ml just prior to FACS analysis and analyzed for FL-2 (488 excitation, 575/26 emission). Sequential analysis of the distinct fluorophores was used and cells with increased PI fluorescence (loss of membrane integrity) were excluded during the analysis. Cell debris or fragments were gated out from the analysis on a forward scatter/side scatter plot. The appearance of discrete cell populations was identified as described previously (13). Briefly, gates were set on dot plots of the respective dye-fluorescence *versus* forward scatter, and then represented accordingly. Changes in the biochemical parameters during apoptosis are observed as changes in the normal distribution of the population of cells with differences in the mean fluorescence intensity for the distinct fluorescent reporters used, compared with control cells in the absence of stimuli and were determined as follows.

Changes in Intracellular Glutathione Content, GSH_i

For intracellular GSH determinations, cells were preloaded for 15 min with 10 μM mBCl, which forms blue fluorescent adducts with intracellular glutathione (30). Immediately prior to flow cytometry examination, PI was added. For mBCl, cells were excited with a Violet (UV) 405 nm laser, and emission was acquired with a 440/40 filter. Changes in the GSH_i are reflected by the appearance of populations of cells with differences in mBCl fluorescence, reflecting changes in GSH_i. Populations were gated as previously described (13). Briefly, contour plots of mBCl fluorescence *versus* forward scatter were used to identify populations of cells with different GSH_i levels induced after FasL treatment. Three different cell populations were identified and represented independently.

Detection of Reactive Oxygen Species (ROS)

Hydrogen peroxide formation was detected using nonfluorescent DHR, which after its oxidation by H_2O_2 in the presence of peroxidases, or Fe^{2+} results in cationic rhodamine (31). Hydroxyl radical ($^{\bullet}OH^{-}$) formation was analyzed using HPF, which is essentially

nonfluorescent until it reacts with •OH yielding a bright green fluorescent compound (32). Nitric oxide (NO) detection was performed using DAF-FM diacetate (4-amino-5-methyl-amino-2′,7′-difluorofluorescein diacetate). After its cleavage by intracellular esterases, DAF is nonfluorescent until it reacts with the spontaneous oxidation product of nitric oxide, nitrosonium cation, to form a fluorescent heterocycle benzotrizole that is trapped in the cytosol. Cells were preloaded for 30 min with 5 μM of either DHR, HPF, or DAF-FM and analyzed for FL1 (488 excitation, 530/30 emission).

Generation of lipid peroxides (LPO) was assessed using BODIPY® FL EDA, which upon interaction with peroxyl radicals looses its fluorescence; and also by fluorescence quenching of the fatty acid analog CsPA (33). Cells were equilibrated with either 5 μM BODIPY® FL EDA or 1.5 μM CsPA for 30 min. Then, cells were washed and resuspended in fresh medium before apoptosis induction. BODIPY® FL EDA was analyzed in FL-1 and CsPA was analyzed at 325/355 nm (ex) and 440/40 (em). Superoxide anion ($^{\bullet}O_2^-$) formation was detected using DHE, which after its oxidization to ethidium by $^{\bullet}O_2^-$, it intercalates within the DNA and exhibits bright red fluorescence (34). Cells were preloaded for 30 min with 5 μM DHE, and changes in its fluorescence were detected in FL-2. For DHE analysis, TOTO-3 dye was added to the samples instead of PI and analyzed at 633 excitation and 660/20 emission to assessed loss of membrane integrity.

Caspase 3 and PARP Cleavage Analysis by FACS

Simultaneous analysis of the cleavage of caspase 3 and PARP was performed as previously described (13). Briefly, cells were washed with phosphate-buffered saline (PBS), then fixed and permeabilized using the Cytofix/Cytoperm kit for 30 min at room temperature in the dark according to the manufacturer's specifications. Cells were then pelleted and washed with the Perm/Wash buffer and stained for 1 h at room temperature in the dark with FITC-conjugated anti-active caspase 3 or PE-conjugated anti-PARP cleavage site-specific. Following incubation, cells were washed with the Perm Wash buffer and analyzed by flow cytometry. PE and FITC fluorescence were examined using an Argon 488 laser with 575/26 and 530/30 filters, respectively.

Analysis of Plasma Membrane Lipid Symmetry

Changes in the phosphatidylserine symmetry were determined using annexin V conjugated to FITC (Trevigen, Gaithersburg, MD). Briefly, 5×10^5 control or treated cells, initially washed in PBS, were incubated with 1 μl of annexin-FITC and PI for 15 min at room temperature according to the manufacturer's instructions. Annexin-FITC/PI-stained samples were diluted in 400 μl of 1× annexin binding buffer and examined immediately by FACS. FITC fluorescence was analyzed on FL1. Early apoptotic cells are defined as having annexin positive, propidium iodide negative staining. Late apoptotic and non-viable cells are both annexin and propidium iodide-positive.

Differential Interference Contrast (DIC) Microscopy

A Zeiss LSM 510 microscope (One Zeiss Drive, Thornwood, NY) was used to obtain DIC images. Cells were prestained for 30 min at 37 °C and 5% CO_2 with 5 μg/ml of Hoechst 33342 and then washed with fresh culture media. Hoechst-stained cells were examined with a Plan-Apo 63 × oil N.A. = 1.4 objective lens to obtain simultaneous DIC and UV images. Hoechst was excited at 390 nm with a Titanium Sapphire 750 nm laser, and emission was collected with a BP 465 filter. Images were analyzed with LSM 5 image browser software.

Extracellular GSH and GSSG Determinations

Extracellular GSH determinations were performed as described in Ref. 13 with minor modifications to improve GSH recovery. Experiments were performed in Hanks' balanced salt solution (SIGMA/Aldrich). Cells were incubated with 250 μM L-(α*S*,5*S*)-α-amino-3-chloro-4,5-dihydro-5-isoxazoleacetic acid (acivicin) for 1 h, to inhibit catabolism-released GSH by the γ-glutamyltransferase (GGT). Then, cells (2×10^7 cells/ml) were induced to undergo apoptosis with FasL. This allowed an improved recovery of accumulated extracellular GSH. Acivicin was present throughout the experiment. Samples were centrifuged, and aliquots were taken for extracellular determinations. Pellets were resuspended in ice-cold phosphate-buffered saline, homogenized, and kept frozen until use for protein determinations. The extracellular GSH and GSSG concentrations were measured enzymatically using the GSH/GSSG-412 kit (Oxis Research, Portland, OR). Samples were prepared in 5% metaphosphoric acid to remove proteins, with or without 1-methyl-2-vinyl-pyridium trifluoromethane sulfonate, a GSH-specific scavenger. Ellman's reagent (5′,5-dithiobis-2-nitrobenzoic acid) reacts with GSH to form a product with an absorption maximum at 412 nm. GSSG was determined using glutathione reductase and β-nicotinamide adenine dinucleotide phosphate (NADPH) to reduce GSSG to GSH followed by reaction with Ellman's reagent. Results are normalized to protein concentration for each sample.

[^{3}H]GSH Uptake Assays

Apoptosis was induced in the presence of 1 μCi of [^{3}H] GSH ([*glycine*-2-^{3}H]glutathione, 1.53 TBq/mmol, Perkin Elmer, Boston, MA). The experiments were done in the presence of 250 μM acivicin and 1 mM BSO (DL-buthionine-(*S,R*)-sulfoximine) to inhibit both GSH catabolism and *de novo* synthesis, respectively. At the indicated time, cells were separated from the medium by filtering through a glass micro-fiber filter (Whatman). Filters were washed with ice-cold PBS. Then, the filter was dried and placed in a scintillation vial containing 10 ml of Ecolite (ICN Radiochemicals, Costa Mesa, CA). The radioactivity was counted in a LS6500 scintillation counter (Beckman Coulter, Fullerton, CA). Results are expressed as the radioactivity incorporated (dpm) normalized to protein concentration.

Protein Extraction and Western Immunoblotting

Cells were pelleted, washed once with ice-cold PBS, and lysed in buffer containing 20 mM Tris-HCl, 150 mM NaCl, 1 mM Na_2EDTA, 1 mM EGTA, 1% Triton X-100, and protease inhibitors (Complete Mini protease mixture, Roche). Samples were sonicated, centrifuged, and the pellets discarded. Then, samples were assayed in a Beckman DU650 spectrophotometer for protein concentration using Bio-Rad protein assay, and cell extracts were normalized to equal protein concentration. Loading buffer containing glycerol, sodium dodecyl sulfate (SDS), and bromphenol blue was added, and samples were denatured at 99 °C for 5 min. Protein extracts, 50 μg/sample, were separated by SDS-polyacrylamide gel electrophoresis (PAGE) on 4–20% gradient polyacrylamide Tris/glycine gels (Novex, Invitrogen, CA) and transferred to nitrocellulose. Membranes were blocked in Tris-buffered saline (TBS) containing 0.1% Tween and 10% nonfat dry milk for 1 h. Antibodies were diluted in TBS containing 0.1% Tween and 5% nonfat dry milk. Blots were incubated with the corresponding primary antibody (1:1000) overnight. Then, blots were incubated for 1 h with the corresponding horseradish peroxidase-linked secondary antibodies (Amersham Biosciences) diluted 1:10,000 in TBS containing 0.05% Tween, and 0.5% nonfat dry milk. Blots were then visualized on film with the ECL chemiluminescent system (Amersham Biosciences). Blots were subsequently stripped using 65 mM Tris-HCl, pH 6.7, 100 mM β-mercaptoethanol, 2% SDS buffer, and reprobed with distinct antibodies. To verify equal protein loading, blots were also reprobed with anti-α-tubulin antibody.

Statistical Analysis

When indicated, significance of differences in mean values were calculated using the two-tailed Student's *t* test. The number of experiments is indicated in each case in the legends of the figures.

RESULTS

FasL-induced GSH Loss Is Independent of, but Necessary for, the Generation of ROS

Glutathione depletion is a common phenomenon during apoptosis (11–14). Most studies suggest that GSH depletion during apoptosis is an indicator for ROS formation and oxidative stress. Such findings have led to the widespread assumption that GSH depletion is a byproduct of the apoptotic process; and that ROS formation and GSH depletion in apoptosis are coupled together as cause and consequence phenomena (6,7,35). However, we and others (11–13,15, 16) have demonstrated that GSH loss is mediated by the activation of a specific efflux pump. Triggering apoptosis induces the formation of ROS and RNS (6,7,35). Thus, we sought to investigate the relationship between GSH depletion and ROS formation in FasL-induced apoptosis in Jurkat cells. Because of the stochastic nature of apoptosis, multiparametric flow cytometry (FACS) was used because it allows us to identify the appearance of discrete populations of cells at different stages in apoptosis and to analyze them at the single cell level. Such analysis is not possible with conventional bulk biochemical assays. Fig. 1 (*histograms*) shows that FasL induced a dose-dependent generation of several ROS forms including H_2O_2 (Fig. 1*A*), superoxide anion $^{\bullet}O_2^-$ (Fig. 1*B*), hydroxyl radical $^{\bullet}OH$ (Fig. 1*C*). We also detected lipid peroxide (LPO) formation (Fig. 1*D*), observed as a loss of BODIPY FL-EDA-fluorescence because of its oxidation. Simultaneous analysis of changes in GSH content and ROS demonstrate that ROS formation was concomitant with GSH depletion (Fig. 1, *A–D*, *contour plots*). To detect the generation of H_2O_2 we used DHR, which has proved to be a more stable dye for H_2O_2 detection (32,36). Although DHR can also be oxidized by peroxynitrite ($OONO^-$) (31), ebselen (10–100 μM), a cell permeable scavenger of $OONO^-$, did not inhibit DHR oxidation during FasL-induced apoptosis, suggesting that changes in DHR reflect changes in H_2O_2 content. We did not detect singlet oxygen ($^1O_2$) (assessed with the Singlet Oxygen Sensor Green dye), or nitric oxide (NO) (analyzed using the nitric oxide dye DAF-FM) formation during FasL-induced apoptosis (data not shown). Reactive oxygen species generation occurred in all cases, prior to the loss of membrane integrity assessed by changes in PI fluorescence.

We next analyzed the role of ROS on the modulation of GSH depletion by the use of a variety of antioxidants (Fig. 2, *A–C*). Hydrogen peroxide formation induced by FasL was prevented in the presence of pyruvate (Fig. 2*A*, *upper panels*), which acts as a potent intracellular scavenger for H_2O_2 (37–39). Superoxide anion formation was drastically reduced by the cell permeable manganic-porphyrins MnTE-2-PyP (Fig. 2*B*, *upper panels*) and MnTBAP, which act as a superoxide dismutase (SOD) mimic, but not by the inhibitor of the NADPH oxidase, DPI (50 μM) (data not shown). In addition, dimethyl sulfoxide, which quenches $^{\bullet}OH$ to form the stable nonradical compound methanosulfinic acid, significantly decreased $^{\bullet}OH^-$ formation (Fig. 2*C*, *upper panels*). Finally, supplementation of cells with trolox, a cell-permeable vitamin E analog, which is known to be a potent lipophilic scavenger of lipid peroxides, prevented LPO formation (Fig. 2*D*, *upper panels*). Similar results were also observed when we used CsPA to analyze LPO formation (data not shown). Reduced glutathione has been reported to scavenge directly or indirectly many of these and other ROS forms. However, scavenging of the ROS generated upon Fas activation by these antioxidants, did not significantly affect GSH depletion (Fig. 2, *A–D*, *lower panels*) corroborating that GSH depletion is not related to its oxidation. As reported previously, supplementation with trolox, significantly reduced cellular GSH content (40) (Fig. 2*D*).

The studies described above led us to consider: 1) whether GSH depletion was required for ROS formation; and 2) whether ROS subsequently mediated the reported regulatory effects of GSH depletion in apoptosis. Our previous study demonstrated that GSH loss during FasL-induced apoptosis is prevented by decreasing the electrochemical gradient of GSH across the plasma membrane with high extracellular GSH medium (13). High extracellular GSH medium significantly reduced the generation of all ROS formed during FasL stimuli (Fig. 3). A comparable degree of prevention of ROS formation was observed in the presence of NAC, a thiol dipeptide that replenishes intracellular GSH content. These data strongly indicate that GSH depletion is necessary for ROS generation and that this depletion precedes cellular oxidative stress. We have previously demonstrated that MK571 is a potent stimulator of GSH depletion during apoptosis (13). Fig. 4 shows that stimulation of GSH loss by MK571 was paralleled by an increase in oxidative stress measured by an increase in the levels of $^{\bullet}O_2^-$. These data suggest that GSH depletion regulates oxidative stress during apoptosis.

Reactive Oxygen Species Generation Is a Bystander Phenomenon That Does Not Regulate FasL-induced Apoptosis in Jurkat Cells

We have recently demonstrated that GSH depletion is necessary for the activation of the execution phase of apoptosis (13). The role of ROS in apoptosis has been largely implicated by the use of agents that by themselves stimulate ROS formation. However, the involvement of ROS in apoptosis induced by physiological stimuli remains controversial (41). Because we observed that GSH depletion preceded ROS formation, we sought to determine if ROS modulates apoptosis induced by FasL. Fig. 5*A* shows that FasL-induced apoptosis, measured by phosphatidyl externalization and loss of plasma membrane integrity (cell viability), was not affected in the presence of any of the antioxidants demonstrated to inhibit ROS formation. Similarly, FasL induced cleavage of caspase 3 and PARP simultaneously analyzed by FACS, as well as other morphological parameters of apoptosis including nuclear condensation, plasma membrane blebbing, and cellular fragmentation were not affected by the non-thiol antioxidants tested (Fig. 5, *B* and *C*). To evaluate the possibility that quenching one ROS is compensated by other ROS formed, and so their possible role on GSH loss and apoptosis is underestimated, we assessed the effect of an antioxidant mixture (ANT-CK), which contained pyruvate, MnTE-2-PyP, Me_2SO, and trolox at the concentrations used to individually quench each ROS, on apoptosis induced by Fas activation. The ANT-CK did not prevented the appearance of any of the apoptotic markers examined (Fig. 5). We also analyzed the effect of other antioxidants for distinct ROS and RNS. Singlet oxygen is another highly reactive free radical, which acts as a common intermediate in a range of biological systems exposed to oxidative stress. Moreover, singlet oxygen has shown to be generated in other biological processes that do not involve light (42). The RNS, NO, and $OONO^-$ have also been reported to act as important modulators of apoptosis (43,44). Neither the antioxidants for NO and $OONO^-$, carboxy-PTIO (100 μM), and ebselen (10–100 μM), nor the $^1O_2$ scavenger, sodium azide (NaN_3, 10 mM), had an effect on FasL-induced GSH loss and apoptosis when used alone or in combination with the ANT-CK (data not shown). Thus, FasL-induced apoptosis in Jurkat cells is clearly independent from increases in ROS formation.

Previous studies have reported a protective effect of several other antioxidants such as catalase and deferoxamine on apoptosis induced by Fas activation (22,25,45). However, little effectiveness of these antioxidants was observed in our experimental model. Fig. 6, *A* and *B* shows that catalase and deferoxamine do not scavenge the increase in H_2O_2 and $^{\bullet}OH^-$ formation induced by FasL. Moreover, they did not prevent GSH depletion and apoptosis under the same conditions (Fig. 6, *A*–*D*). The lack of effect of these antioxidants in our system, particularly on the scavenging of ROS, is more consistent with a limited cell permeability of these agents. Catalase (a 240-kDa enzyme that catalyzes H_2O_2 to water and oxygen) does not permeate the cells unless plasma membrane integrity is compromised. Similarly, deferoxamine

is a lysosomotropic iron chelator, which has been demonstrated to be impermeable to the plasma membrane and if internalized, has been shown to be uptaken by endocytosis and exclusively localized in the cells at the lysosome compartment (46–48). This discrepancy likely relies on the different cell types used (22,25,45). Medan *et al.* (25) reported that when they used macrophages, catalase and deferoxamine efficiently scavenge ROS and prevent apoptosis induced by Fas activation. This is probably ascribed to the phagocytic potential of macrophages that might efficiently accumulate these antioxidants. In our studies, we used pyruvate that has been reported be actively uptaken by monocarboxylate transporters by cells and to act as a potent intracellular scavenger for H_2O_2 (37–39). Similarly, dimethyl sulfoxide freely permeates the plasma membrane and directly quenches $^{\bullet}OH^{-}$. Other antioxidants tested here, such as a superoxide dismutase mimic (MnTBAP) and vitamin E (trolox), to scavenge $^{\bullet}O_2^{-}$ and LPO, were also used in their cell-permeable form to ensure effective ROS scavenging as shown in Fig. 2.

Glutathione Transport Regulates Apoptosis Induced by Multiple Stimuli

We and others (11–13,15) have recently shown that the reduction in the GSH content during apoptosis in Jurkat cells is mediated through the activation of an efflux transport mechanism rather than due to its oxidation to GSSG or to the loss of membrane integrity. We recently showed that this transport is stimulated by distinct agents including MK571 and is inhibited by high extracellular GSH concentrations. Fig. 7*A* shows that indeed, FasL-induced GSH depletion is stimulated by MK571 and prevented by high GSH medium. The same stimulatory effects are observed by other OA^{-} substrates including taurocholic acid and estrone sulfate (data not shown). We have previously demonstrated that MK571 is a more potent stimulator of GSH depletion during apoptosis (13). In accordance with our previous work (13), FasL-induced extracellular GSH accumulation was significantly stimulated by MK571 (Fig. 7*B*). A slight, but significant accumulation of oxidized GSH in its disulfide form (GSSG) was also detected extracellularly, which might be ascribed to GSH oxidation after its release.

We next evaluated whether GSH efflux and depletion is a necessary for the progression of apoptosis induced by different apoptotic stimuli known to activate cell death via distinct signaling pathways. Fig. 8*A* shows that FasL-induced apoptosis observed as phosphatidylserine externalization (Fig. 8*A*), nuclei condensation, plasma membrane blebbing, and cell fragmentation (Fig. 8*B*), was prevented by inhibition of GSH depletion by high extracellular GSH. In contrast, stimulation of GSH depletion with MK571 accelerated the progression of cell death. Additionally, high extracellular GSH medium prevented apoptosis induced by other stimuli including stress (UVC radiation), impairment of protein synthesis (cycloheximide), and inhibition of topoisomerase II (etoposide) (Fig. 8*C*). Together these results suggest that the regulation of cell death progression by changes in GSH content is a common component of apoptosis induced by a variety of signals that activate both intrinsic and extrinsic pathways of cell death.

N-Acetyl-cysteine is a derivative of the sulfur-containing amino acid cysteine and an intermediary (along with glutamic acid and glycine) in the conversion of cysteine to GSH. NAC is thought to be transported into the cell directly where it is hydrolyzed to cysteine before it serves as a precursor for GSH formation. In the presence of NAC, FasL-induced GSH depletion was prevented (Fig. 9*A*). Replenishing of the intracellular GSH pools with the thiol dipeptide NAC also protected Jurkat cell from apoptosis induced by FasL analyzed by phosphatidyl-serine externalization (Fig. 9*B*); nuclei condensation, plasma membrane blebbing, and cell fragmentation (Fig. 9*D*); and cleavage of execution caspases 3,6, and 7 and of their substrates PARP and α-fodrin (Fig. 9, *C* and *E*). Moreover, the enhancement of apoptosis by MK571-induced stimulation of GSH depletion was fully prevented by NAC (Fig. 9).

It is still controversial how extracellular GSH influences cellular redox state. In contrast to NAC, GSH is thought to be taken up poorly by cells, and thus it only serves to provide constituent amino acids. Indeed, GSH has to be broken down into its constituent amino acids, transported into the cell, and then resynthesized *de novo* catalyzed by the activity of the γ-glutamylcysteine synthetase (γ-GCS). We next studied the mechanism for extracellular GSH to maintain the level of intracellular GSH and reduce Fas-mediated apoptosis. To asses the role of *de novo* synthesis of GSH in this process, we evaluated the protective effect of high extracellular GSH in the presence of BSO, an inhibitor of the γ-GCS. A 24-h treatment with BSO significantly depletes cells of intracellular GSH (−GSH) (Fig. 10*A*). When GSH-depleted cells were preincubated with high GSH medium the intracellular GSH pool is significantly replenished after 4 h, even with persistent inhibition of *de novo* GSH synthesis pathway with BSO. Fig. 10*B* shows that high extracellular GSH stimulates an active uptake of radiolabeled [^{3}H]GSH in the presence of BSO. These results suggest that high extracellular GSH is able to replenish the intracellular GSH pool without the involvement of *de novo* synthesis; thus, suggesting an influx of extracellular GSH. Finally, high extracellular GSH was still able to prevent FasL-induced GSH depletion (Fig. 10*C*) and apoptosis induced by FasL, analyzed by phosphatidylserine externalization (Fig. 10*D*); cleavage of execution caspases 3 and PARP (Fig. 10*E*); and nuclei chromatin condensation, plasma membrane blebbing, and cell fragmentation (Fig. 10*E*), even when GSH *de novo* synthesis was inhibited by BSO. These results suggest that high GSH concentrations might protect against apoptosis by reversing GSH efflux transport and not by replenishing GSH pools via *de novo* synthesis.

DISCUSSION

The redox environment of the cells has been suggested to be important in the control of apoptosis. Small thiols, including glutathione are viewed as protective antioxidants acting as free radical scavengers in response to oxidative damage; thus, being important players in the redox balance of the cell. Glutathione depletion has been shown to occur in apoptosis induced by a wide variety of stimuli, and has been shown mediated by its extrusion and not its oxidation (11–17). Glutathione depletion has been shown to directly modulate both the permeability transition pore formation, and the activation of execution caspases (13,49–54). *In vitro* studies have also shown that a reduction in the GSH_i is necessary for the formation of the apoptosome (23). We recently demonstrated that GSH depletion during FasL-induced apoptosis is mediated by its extrusion through the activation of a plasma membrane GSH transport mechanism. In addition we demonstrated that GSH efflux is necessary for the activation of the execution phase of FasL-induced apoptosis (13). However, the precise mechanism by which GSH loss regulates apoptosis remains unclear. Because GSH depletion and ROS generation are both phenomena largely thought to be correlated, we sought to clarify the relationship between ROS and GSH depletion during FasL-induced apoptosis. Here, we present evidence that shows not only that GSH depletion is independent of ROS generation, but that ROS formation is most likely a bystander phenomenon in the progression of FasL-induced apoptosis in lymphoid cells. We propose that thiol regulation of apoptosis is largely independent of ROS formation. Finally, GSH depletion was observed to be necessary for the progression of apoptosis induced by several different stimuli, which act by different signaling pathways to induce cell death.

We previously reported that GSH efflux in FasL induced apoptosis is mediated, by a transporter with characteristics of a GSH/OA^- exchanger (13). Members of the SLCO/OATP transporter family have been suggested to function as bidirectional transporters of glutathione in exchange for an organic anion (OA^-) substrate (55–62) acting then, as GSH exchangers. In addition, they are reported to transport a wide range of OA^- in exchange for GSH (56,59). Glutathione efflux by these proteins has been reported to be trans-stimulated by extracellular OA^- substrates (*i.e.* its transport is accelerated by the presence of extracellular substrates that increase the exchange transport rate). The driving force for the net GSH export through GSH/OA^-

exchangers is determined by the electrochemical gradient of GSH across the plasma membrane (11,59). Glutathione is 90% freely distributed in the cytosol where it is present in concentrations up to 10 m_M in animal cells, whereas in plasma, concentrations are ~0.01 m_M, and in cell culture medium they are around 0.003 m_M. Moreover, because GSH is negatively charged at physiological pH, there is a large intracellular negative potential of −30 to −60 mV that facilitates its extrusion. Increasing the extracellular GSH concentration decreases the driving force of GSH extrusion and reduces net GSH efflux mediated by GSH/OA^- exchangers. Thus, high extracellular GSH should stimulate GSH/OA^- exchange of GSH_i; however, net reduction of GSH_i is prevented by its exchange for extracellular GSH.

Bi-directional GSH/OA^- has been reported in different cell types including human cell lines (56,57,60–64). Although OATP (human)/Oatp (rat, mouse) proteins were initially reported to mediate this exchange transport (57,58,62), a recent study has suggested that GSH/OA^- exchange is not mediated by this family of transporters (65,66). We have previously detected the presence of mRNA for 7 different members of the *SLCO*/OATP family of transporters in Jurkat cells (13). We have initially proposed that an exchange transporter mediates GSH efflux during apoptosis based on several characteristics: 1) stimulation by a wide variety of extracellular OA^- substrates including MK571; 2) reduction by high extracellular GSH medium independent of *de novo* synthesis; thus, suggesting that high extracellular GSH medium reverses GSH efflux during apoptosis by reducing its electrochemical gradient across the plasma membrane; and 3) activation of an OA^- influx that parallels GSH efflux (13).

Other studies have suggested that ABCC/MRP transporters may be involved in GSH efflux during apoptosis (16,67,68). In contrast to our observations, Ballatori and co-workers recently reported that inhibitors of MRP transport including MK571 prevent GSH loss and apoptosis in Jurkat cells. This discrepancy between the two studies is likely explained by the fact that the Ballatori and co-worker experiments were performed under a glucose-depleted condition, which is an apoptotic stimulus by itself. In addition, their bulk assays used to asses both apoptosis and changes in GSH_i cannot discriminate between apoptotic and necrotic cells. Because apoptosis is a stochastic cellular process, we have analyzed these events at the single cell level by flow cytometry. Whether GSH efflux during apoptosis is mediated by OATP, MRP, or any other still unidentified transporter remains to be clarified.

The progression of apoptosis has been largely reported to correlate with the generation of ROS and RNS (7). Glutathione contributes to key antioxidant metabolic pathways by acting either as a proton donor, or as the cofactor for nucleophilic conjugation and thus, it has been shown to scavenge a wide range of ROS and RNS. While GSH scavenges $^{\bullet}O_2^-$, $^{\bullet}OH$, $^1O_2$, and NO directly, it catalytically detoxifies cells from hydroperoxides (H_2O_2), $OONO^-$, and lipid peroxides by the action of glutathione peroxidases. Because glutathione is the major intracellular antioxidant defense within the cells, we propose that its depletion might be a prerequisite for the generation of ROS that could potentially modulate the apoptotic machinery. We show that inhibition of GSH depletion by either high extracellular GSH or NAC abolishes the increase in ROS formation. Moreover, we observed a tight link between GSH transport and ROS formation because ROS generation was stimulated by MK571 a potent stimulator of GSH efflux during FasL-induced apoptosis (13).

The role of ROS in the progression of the cell death program induced by FasL is controversial. While previous studies suggested a role of ROS in apoptosis (22–24), contradictory results have also been described (27,28,69–71). Previous reports have studied the role of one particular ROS in apoptosis; however, the formation or even scavenging of one ROS can potentially lead to the generation of others by different reactions. FasL-mediated apoptosis has been reported to induce the generation of H_2O_2 (20,22,24–26,45,72,73), $^{\bullet}O_2^-$ (22,23,73–78). OH^- (25), NO (79), and lipid peroxides (80,81). During apoptosis, $^{\bullet}O_2^-$ has been specifically shown to be

formed due to a switch from 4-electron reduction of O_2 to a 1-electron reduction (7,82). Superoxide anion can be subsequently converted to H_2O_2 or $^1O_2$, by non-enzymatic reactions. Furthermore, $^{\bullet}O_2^-$ can be derived enzymatically to H_2O_2 from its dismutation by SOD. Reaction of H_2O_2 with $^{\bullet}O_2^-$ in the presence of iron can further produce $^{\bullet}OH$ by Fenton-type reactions (83). The hydroxyl radical can trigger a chain of peroxidation reactions by subtracting allylic hydrogen atoms from proximal unsaturated lipids (84), which is highly toxic to the cell because a single ROS can generate a number of toxicants because of the autocatalytic propagation of lipid peroxidation reactions. We observed an example of this interrelationship of one ROS generation with others when in the presence of the SOD mimic MnTE-e-PyP, which prevents $^{\bullet}O_2^-$ formation upon Fas stimulation, H_2O_2 formation was enhanced as a byproduct of $^{\bullet}O_2^-$ dismutation (data not shown). We took an integrative approach by analyzing the role of several reactive species in apoptosis, by the use of several antioxidants alone or in conjunction. Scavenging of H_2O_2, $^{\bullet}O_2^-$, $^{\bullet}OH$, and LPO formed upon Fas stimulation, neither regulate GSH loss, nor protect from the progression of apoptosis. Moreover, the presence of antioxidants stimulated FasL-induced apoptosis which is in accordance with other reports that suggested an inhibitory role of distinct ROS during cell death (27,28,69–71). To eliminate the possibility that the role of ROS in apoptosis was masked or underestimated by a possible compensation of other ROS, we analyzed the combined effect of several antioxidants as a mixture. The antioxidant mixture tested did not protect against apoptosis upon FasL stimuli. Other antioxidants for $^1O_2$, NO, and $ONOO^-$ when administered alone or in conjunction with others also had no effect on apoptosis. These results suggest that the increases in the formation of reactive species during FasL-induced apoptosis do not regulate GSH loss or cell death.

Many reports have proposed a role for ROS in death receptor-mediated apoptosis, particularly during Fas-mediated apoptosis (20,22–26,45,72–78,85,86). Antagonistic roles for ROS have on the other hand, also been reported (27–29,69,87–92). The role of ROS in Fas-induced apoptosis has been suggested previously by the protective effect of the extracellular addition of thiols (GSH or NAC) on cell death progression, although the effects have been largely ascribed to the well known capacities of thiol compounds as antioxidants (22,23,72,78,93, 94). We have observed here that high extracellular GSH and NAC, both of which prevent GSH depletion, protect Jurkat cells from undergoing apoptosis induced by death receptor activation (FasL), stress (UVC radiation) and drugs (cycloheximide and etoposide). In contrast, other equally effective antioxidants that prevented ROS formation upon FasL stimuli, used alone or in conjunction, had no effect on apoptosis. Thus, we conclude that inhibition of apoptosis by using any experimental approach that prevents GSH depletion or replenishes cellular GSH levels cannot be used as an indicator of a role of reactive species in apoptosis, but rather as evidence of a regulatory role of changes in GSH content. This hypothesis is supported by previous observations showing that apoptosis can occur under anaerobic conditions, *i.e.* in the absence of ROS formation (41); or in cells deficient in respiration and mitochondrial oxidative phosphorylation (95), which is the source of ROS during apoptosis (7,82,96). Moreover, in peripheral T-lymphocytes protection from apoptosis by thiol-compounds is observed in the absence of any ROS formation (93). These observations are important in the sense that they indicate, a regulatory role for changes in GSH content during apoptosis independent from ROS, and they explain contradictory results on the protective effects of thiol and non-thiol antioxidants in apoptosis.

Thus, we show that the generation of ROS and oxidative stress upon FasL stimuli do not regulate the progression of apoptotic cell death. However, the exact mechanism involved in the modulation of apoptosis by GSH depletion remains unclear. Although the role of GSH in distinct cell processes has been mainly ascribed to its potent antioxidant properties, GSH might modulate apoptosis by other distinct mechanisms. Thiol/disulfide exchange reactions at the level of cysteine residues in proteins involved in the apoptotic cascade have been recently

suggested to regulate the progression of apoptosis (93,97). Thus, GSH loss might be regulating apoptosis involve post-translational modifications of apoptotic enzymes by thiol exchange reactions. Thiol exchange reactions might also be involved in the regulation of ion channels and changes in the ionic homeostasis of the cell (4,5,98) that are known to regulate the activation of caspases and endonucleases (4,5,98). More studies are necessary to elucidate the exact mechanism or mechanisms involved in GSH depletion mediated regulation of apoptosis.

Acknowledgments

We thank Dr. John B. Pritchard and Dr. Ronald P. Mason for the internal review and comments on this manuscript. We thank Jeff Reece and Jeff Tucker for technical support in the DIC microscopy, and Maria Sifre for assistance with the FACS experiments.

REFERENCES

1. Green DR. Immunol. Rev 2003;193:5–9. [PubMed: 12752665]
2. Fadeel B, Orrenius S. J. Intern. Med 2005;258:479–517. [PubMed: 16313474]
3. Brunner T, Wasem C, Torgler R, Cima I, Jakob S, Corazza N. Semin. Immunol 2003;15:167–176. [PubMed: 14563115]
4. Bortner CD, Cidlowski JA. Cell Death Differ 2002;9:1307–1310. [PubMed: 12478467]
5. Franco R, Bortner CD, Cidlowski JA. J. Membr. Biol 2006;209:43–58. [PubMed: 16685600]
6. Carmody RJ, Cotter TG. Redox. Rep 2001;6:77–90. [PubMed: 11450987]
7. Chandra J, Samali A, Orrenius S. Free Radic. Biol. Med 2000;29:323–333. [PubMed: 11035261]
8. Hammond CL, Lee TK, Ballatori N. J. Hepatol 2001;34:946–954. [PubMed: 11451183]
9. Wu G, Fang YZ, Yang S, Lupton JR, Turner ND. J. Nutr 2004;134:489–492. [PubMed: 14988435]
10. Roederer M, Staal FJ, Anderson M, Rabin R, Raju PA, Herzenberg LA, Herzenberg LA. Ann. N. Y. Acad. Sci 1993;677:113–125. [PubMed: 8494201]
11. Hammond CL, Madejczyk MS, Ballatori N. Toxicol. Appl. Pharmacol 2004;195:12–22. [PubMed: 14962501]
12. Ghibelli L, Fanelli C, Rotilio G, Lafavia E, Coppola S, Colussi C, Civitareale P, Ciriolo MR. Faseb. J 1998;12:479–486. [PubMed: 9535220]
13. Franco R, Cidlowski JA. J. Biol. Chem 2006;281:29542–29557. [PubMed: 16857677]
14. Beaver JP, Waring P. Eur. J. Cell Biol 1995;68:47–54. [PubMed: 8549589]
15. van den Dobbelsteen DJ, Nobel CS, Schlegel J, Cotgreave IA, Orrenius S, Slater AF. J. Biol. Chem 1996;271:15420–15427. [PubMed: 8662848]
16. He YY, Huang JL, Ramirez DC, Chignell CF. J. Biol. Chem 2003;278:8058–8064. [PubMed: 12502708]
17. Ghibelli L, Coppola S, Rotilio G, Lafavia E, Maresca V, Ciriolo MR. Biochem. Biophys. Res. Commun 1995;216:313–320. [PubMed: 7488106]
18. Friesen C, Kiess Y, Debatin KM. Cell Death Differ 2004;11:S73–S85. [PubMed: 15105835]
19. Watson RW, Rotstein OD, Jimenez M, Parodo J, Marshall JC. Blood 1997;89:4175–4181. [PubMed: 9166861]
20. Kohno T, Yamada Y, Hata T, Mori H, Yamamura M, Tomonaga M, Urata Y, Goto S, Kondo T. J. Immunol 1996;156:4722–4728. [PubMed: 8648118]
21. Chiba T, Takahashi S, Sato N, Ishii S, Kikuchi K. Eur. J. Immunol 1996;26:1164–1169. [PubMed: 8647182]
22. Devadas S, Hinshaw JA, Zaritskaya L, Williams MS. Free Radic. Biol. Med 2003;35:648–661. [PubMed: 12957657]
23. Sato T, Machida T, Takahashi S, Iyama S, Sato Y, Kuribayashi K, Takada K, Oku T, Kawano Y, Okamoto T, Takimoto R, Matsunaga T, Takayama T, Takahashi M, Kato J, Niitsu Y. J. Immunol 2004;173:285–296. [PubMed: 15210786]
24. Perez-Cruz I, Carcamo JM, Golde DW. Blood 2003;102:336–343. [PubMed: 12623840]

25. Medan D, Wang L, Toledo D, Lu B, Stehlik C, Jiang BH, Shi X, Rojanasakul Y. J. Cell Physiol 2005;203:78–84. [PubMed: 15368542]
26. Reinehr R, Becker S, Eberle A, Grether-Beck S, Haussinger D. J. Biol. Chem 2005;280:27179–27194. [PubMed: 15917250]
27. Aronis A, Melendez JA, Golan O, Shilo S, Dicter N, Tirosh O. Cell Death Differ 2003;10:335–344. [PubMed: 12700633]
28. Borutaite V, Brown GC. FEBS Lett 2001;500:114–118. [PubMed: 11445067]
29. Kim H, Kim YN, Kim H, Kim CW. Oncogene 2005;24:1252–1261. [PubMed: 15592513]
30. Sebastia J, Cristofol R, Martin M, Rodriguez-Farre E, Sanfeliu C. Cytometry 2003;51:16–25. [PubMed: 12500301]
31. Gomes A, Fernandes E, Lima JL. J. Biochem. Biophys. Methods 2005;65:45–80. [PubMed: 16297980]
32. Setsukinai K, Urano Y, Kakinuma K, Majima HJ, Nagano T. J. Biol. Chem 2003;278:3170–3175. [PubMed: 12419811]
33. Makrigiorgos GM. J. Biochem. Biophys. Methods 1997;35:23–35. [PubMed: 9310865]
34. Ghelli A, Benelli B, Esposti MD. J. Biochem. (Tokyo) 1997;121:746–755. [PubMed: 9163527]
35. Perl A, Gergely P Jr, Puskas F, Banki K. Antioxid. Redox. Signal 2002;4:427–443. [PubMed: 12215210]
36. Bonini MG, Rota C, Tomasi A, Mason RP. Free Radic. Biol. Med 2006;40:968–975. [PubMed: 16540392]
37. Hinoi E, Takarada T, Tsuchihashi Y, Fujimori S, Moriguchi N, Wang L, Uno K, Yoneda Y. Mol. Pharmacol 2006;70:925–935. [PubMed: 16766717]
38. Ramakrishnan N, Chen R, McClain DE, Bunger R. Free Radic. Res 1998;29:283–295. [PubMed: 9860043]
39. Nakamichi N, Kambe Y, Oikawa H, Ogura M, Takano K, Tamaki K, Inoue M, Hinoi E, Yoneda Y. J. Neurochem 2005;93:84–93. [PubMed: 15773908]
40. Shang F, Lu M, Dudek E, Reddan J, Taylor A. Free Radic. Biol. Med 2003;34:521–530. [PubMed: 12614841]
41. Jacobson MD, Raff MC. Nature 1995;374:814–816. [PubMed: 7536895]
42. Davies MJ. Biochem. Biophys. Res. Commun 2003;305:761–770. [PubMed: 12763058]
43. Virag L, Szabo E, Gergely P, Szabo C. Toxicol. Lett 2003;140–141:113–124.
44. Blaise GA, Gauvin D, Gangal M, Authier S. Toxicology 2005;208:177–192. [PubMed: 15691583]
45. Kasahara Y, Iwai K, Yachie A, Ohta K, Konno A, Seki H, Miyawaki T, Taniguchi N. Blood 1997;89:1748–1753. [PubMed: 9057659]
46. Cable H, Lloyd JB. J. Pharm. Pharmacol 1999;51:131–134. [PubMed: 10217310]
47. Laub R, Schneider YJ, Octave JN, Trouet A, Crichton RR. Biochem. Pharmacol 1985;34:1175–1183. [PubMed: 3994740]
48. Lewandowska H, Meczynska S, Sochanowicz B, Sadlo J, Kruszewski M. J. Biol. Inorg. Chem 2007;12:345–352. [PubMed: 17136409]
49. Armstrong JS, Jones DP. Faseb. J 2002;16:1263–1265. [PubMed: 12060676]
50. Coppola S, Ghibelli L. Biochem. Soc. Trans 2000;28:56–61. [PubMed: 10816099]
51. Haouzi D, Lekehal M, Tinel M, Vadrot N, Caussanel L, Letteron P, Moreau A, Feldmann G, Fau D, Pessayre D. Hepatology 2001;33:1181–1188. [PubMed: 11343247]
52. Ueda S, Nakamura H, Masutani H, Sasada T, Yonehara S, Takabayashi A, Yamaoka Y, Yodoi J. J. Immunol 1998;161:6689–6695. [PubMed: 9862698]
53. Varghese J, Khandre NS, Sarin A. Apoptosis 2003;8:363–370. [PubMed: 12815279]
54. Hall AG. Adv. Exp. Med. Biol 1999;457:199–203. [PubMed: 10500794]
55. Russel FG, Masereeuw R, van Aubel RA. Annu. Rev. Physiol 2002;64:563–594. [PubMed: 11826280]
56. Lee TK, Hammond CL, Ballatori N. Toxicol. Appl. Pharmacol 2001;174:207–215. [PubMed: 11485381]
57. Li L, Meier PJ, Ballatori N. Mol. Pharmacol 2000;58:335–340. [PubMed: 10908301]

58. Hagenbuch B, Meier PJ. Pflugers. Arch 2004;447:653–665. [PubMed: 14579113]
59. Ballatori N, Hammond CL, Cunningham JB, Krance SM, Marchan R. Toxicol. Appl. Pharmacol 2005;204:238–255. [PubMed: 15845416]
60. Garcia-Ruiz C, Fernandez-Checa JC, Kaplowitz N. J. Biol. Chem 1992;267:22256–22264. [PubMed: 1429578]
61. Sze G, Kaplowitz N, Ookhtens M, Lu SC. Am. J. Physiol 1993;265:G1128–G1134. [PubMed: 7904127]
62. Li L, Lee TK, Meier PJ, Ballatori N. J. Biol. Chem 1998;273:16184–16191. [PubMed: 9632674]
63. Ng KH, Lim BG, Wong KP. Kidney Int 2003;63:976–986. [PubMed: 12631078]
64. Iantomasi T, Favilli F, Marraccini P, Magaldi T, Bruni P, Vincenzini MT. Biochim. Biophys. Acta 1997;1330:274–283. [PubMed: 9408181]
65. Mahagita C, Grassl SM, Piyachaturawat P, Ballatori N. Am. J. Physiol. Gastrointest. Liver Physiol. 2007in press
66. Briz O, Romero MR, Martinez-Becerra P, Macias RI, Perez MJ, Jimenez F, San Martin FG, Marin JJ. J. Biol. Chem 2006;281:30326–30335. [PubMed: 16877380]
67. Benlloch M, Ortega A, Ferrer P, Segarra R, Obrador E, Asensi M, Carretero J, Estrela JM. J. Biol. Chem 2005;280:6950–6959. [PubMed: 15561710]
68. Hammond CL, Marchan R, Krance SM, Ballatori N. J. Biol. Chem. 2007
69. Clement MV, Stamenkovic I. EMBO J 1996;15:216–225. [PubMed: 8617197]
70. Beltran B, Quintero M, Garcia-Zaragoza E, O'Connor E, Esplugues JV, Moncada S. Proc. Natl. Acad. Sci. U. S. A 2002;99:8892–8897. [PubMed: 12077295]
71. Pardo M, Melendez JA, Tirosh O. Free Radic. Biol. Med 2006;41:1795–1806. [PubMed: 17157182]
72. Um HD, Orenstein JM, Wahl SM. J. Immunol 1996;156:3469–3477. [PubMed: 8617975]
73. Banki K, Hutter E, Gonchoroff NJ, Perl A. J. Immunol 1999;162:1466–1479. [PubMed: 9973403]
74. Malassagne B, Ferret PJ, Hammoud R, Tulliez M, Bedda S, Trebeden H, Jaffray P, Calmus Y, Weill B, Batteux F. Gastroenterology 2001;121:1451–1459. [PubMed: 11729124]
75. Gendron MC, Schrantz N, Metivier D, Kroemer G, Maciorowska Z, Sureau F, Koester S, Petit PX. Biochem. J 2001;353:357–367. [PubMed: 11139401]
76. Suzuki Y, Ono Y, Hirabayashi Y. FEBS Lett 1998;425:209–212. [PubMed: 9559649]
77. Jayanthi S, Ordonez S, McCoy MT, Cadet JL. Brain Res. Mol. Brain Res 1999;72:158–165. [PubMed: 10529474]
78. Gulbins E, Brenner B, Schlottmann K, Welsch J, Heinle H, Koppenhoefer U, Linderkamp O, Coggeshall KM, Lang F. Immunology 1996;89:205–212. [PubMed: 8943716]
79. Chanvorachote P, Nimmannit U, Wang L, Stehlik C, Lu B, Azad N, Rojanasakul Y. J. Biol. Chem 2005;280:42044–42050. [PubMed: 16246840]
80. Kagan VE, Gleiss B, Tyurina YY, Tyurin VA, Elenstrom-Magnusson C, Liu SX, Serinkan FB, Arroyo A, Chandra J, Orrenius S, Fadeel B. J. Immunol 2002;169:487–499. [PubMed: 12077280]
81. Serinkan BF, Tyurina YY, Babu H, Djukic M, Quinn PJ, Schroit A, Kagan VE. Antioxid. Redox. Signal 2004;6:227–236. [PubMed: 15025924]
82. Cai J, Jones DP. J. Biol. Chem 1998;273:11401–11404. [PubMed: 9565547]
83. Forman HJ, Torres M, Fukuto J. Mol. Cell Biochem 2002;234–235:49–62.
84. Girotti AW. J. Lipid Res 1998;39:1529–1542. [PubMed: 9717713]
85. Gouaze V, Andrieu-Abadie N, Cuvillier O, Malagarie-Cazenave S, Frisach MF, Mirault ME, Levade T. J. Biol. Chem 2002;277:42867–42874. [PubMed: 12221075]
86. Bajt ML, Ho YS, Vonderfecht SL, Jaeschke H. Antioxid. Redox. Signal 2002;4:733–740. [PubMed: 12470500]
87. Hampton MB, Orrenius S. FEBS Lett 1997;414:552–556. [PubMed: 9323034]
88. Tirosh O, Aronis A, Melendez JA. Biochem. Pharmacol 2003;66:1331–1334. [PubMed: 14555205]
89. Clement MV, Hirpara JL, Pervaiz S. Cell Death Differ 2003;10:1273–1285. [PubMed: 12894215]
90. Pervaiz S, Clement MV. Biochem. Biophys. Res. Commun 2002;290:1145–1150. [PubMed: 11811982]

91. Bernassola F, Catani MV, Corazzari M, Rossi A, Melino G. J. Cell. Biochem 2001;82:123–133. [PubMed: 11400169]
92. Hug H, Enari M, Nagata S. FEBS Lett 1994;351:311–313. [PubMed: 7521851]
93. Deas O, Dumont C, Mollereau B, Metivier D, Pasquier C, Bernard-Pomier G, Hirsch F, Charpentier B, Senik A. Int. Immunol 1997;9:117–125. [PubMed: 9043953]
94. Furuke K, Bloom ET. Int. Immunol 1998;10:1261–1272. [PubMed: 9786425]
95. Jacobson MD, Burne JF, King MP, Miyashita T, Reed JC, Raff MC. Nature 1993;361:365–369. [PubMed: 8381212]
96. Ricci JE, Munoz-Pinedo C, Fitzgerald P, Bailly-Maitre B, Perkins GA, Yadava N, Scheffler IE, Ellisman MH, Green DR. Cell 2004;117:773–786. [PubMed: 15186778]
97. Pan S, Berk BC. Circ. Res 2007;100:213–219. [PubMed: 17185628]
98. Bortner CD, Cidlowski JA. Pflugers. Arch 2004;448:313–318. [PubMed: 15107996]

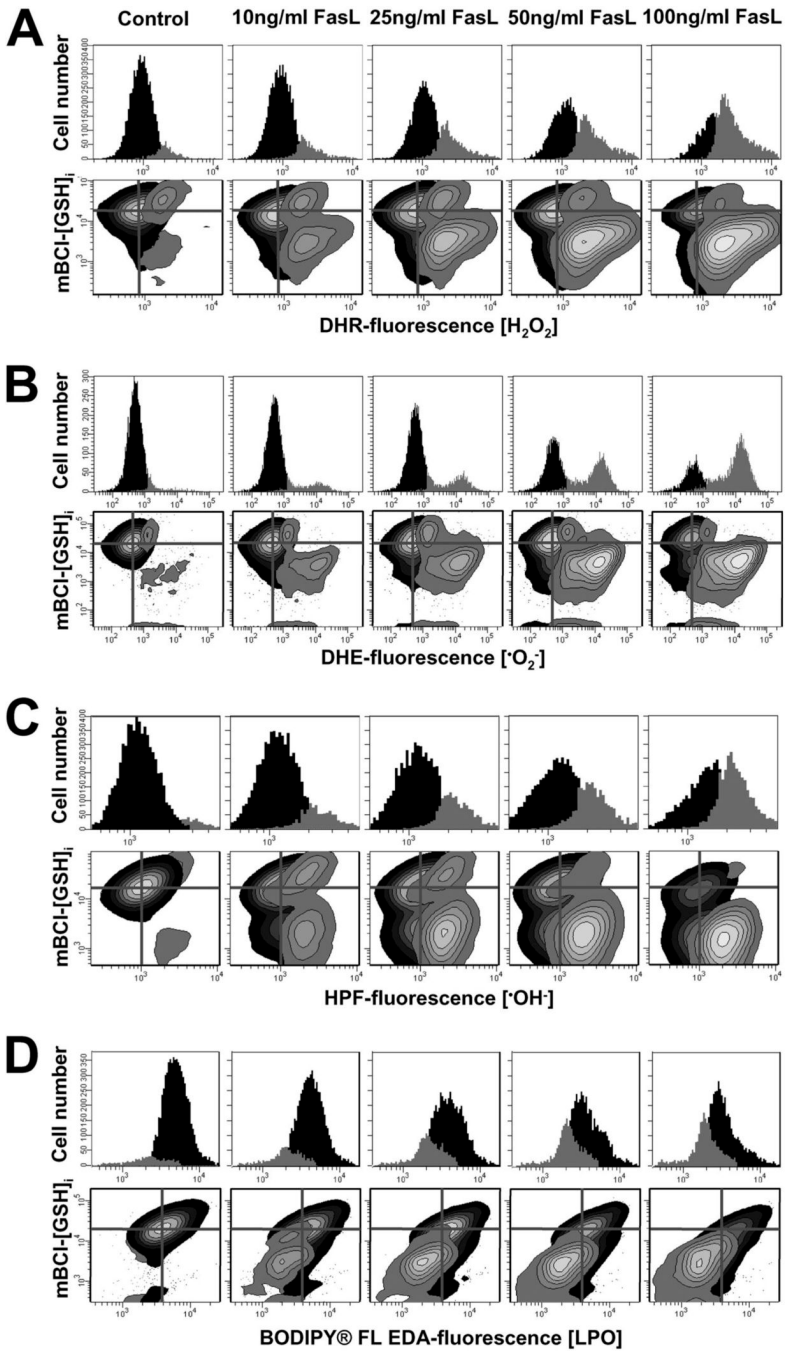

FIGURE 1. Reactive oxygen species generation correlates with changes in intracellular glutathione, GSH_i

Reactive oxygen species formation was assessed by FACS using DHR for H_2O_2 detection; DHE for superoxide anion ($^{\bullet}O_2^-$); HPF for hydroxyl radical ($^{\bullet}OH^-$); and BODIPY® FL EDA, for LPO. Changes in intracellular glutathione concentration GSH_i were determined by FACS using the thiol binding dye monochlorobimane, mBCl. For the induction of apoptosis, Jurkat cells were incubated with FasL for 4 h at the concentration indicated. Data are expressed as changes in ROS-sensitive dye fluorescence represented by frequency histograms (*upper panels in A–D*) or in contour plots *versus* changes in mBCl fluorescence (GSH_i) (*lower panels in A–D*). In contour plots, the quadrant center was set at the mean fluorescence intensity for mBCl

and the corresponding ROS dye, as a reference to indicate basal levels of GSH_i and ROS. Populations were gated and represented according to the differences in ROS levels. Plots are representative of $n = 3$ independent experiments.

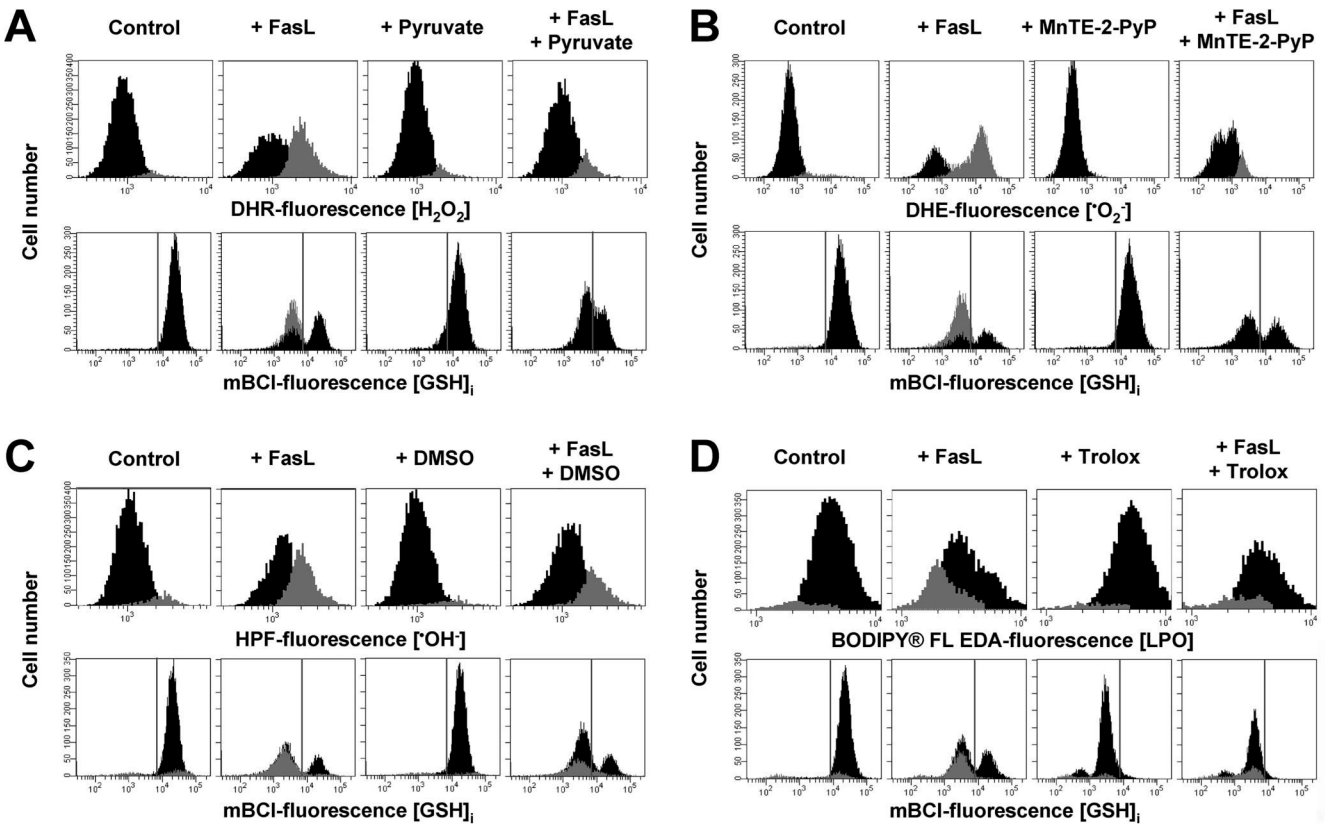

FIGURE 2. Reactive oxygen species scavenging by antioxidants does not affect FasL-induced GSH loss

Reactive oxygen species formation and changes in GSH_i were assessed by FACS. Apoptosis was induced in Jurkat cells by incubation with FasL (50 ng/ml FasL) for 4 h. The effect of the antioxidants 10 mM sodium pyruvate (for H_2O_2) (*A*), 2% Me_2SO ($^{\bullet}OH^{-}$) (*B*), 250 μM MnTE-2-PyP ($^{\bullet}O_2^{-}$) (*C*), and 5 mM trolox (LPO) (*D*), was individually assessed. Jurkat cells were preincubated in RPMI for 1 h at 37 °C with the agents dissolved in either Me_2SO or ethanol, and antioxidants remained throughout the experiment. In all cases, control conditions include vehicles at the same concentration. Populations were gated according to the differences in ROS levels. Data are expressed as frequency histograms of either changes in the fluorescence of the ROS-sensitive dyes (*upper panels A–C*) or mBCl (*lower panels A–C*). In *A–C lower panels*, GSH depletion is depicted as the appearance of a population of cells at the left of the *gray solid lines*. For mBCl fluorescence the *solid line* depicts the plots representative of $n = 3$ independent experiments.

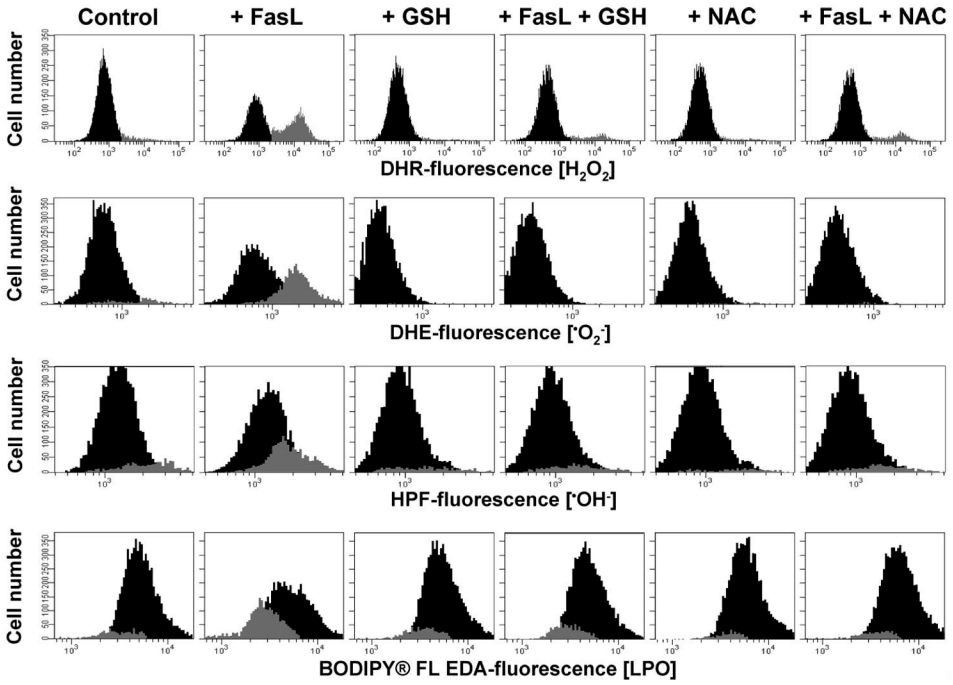

FIGURE 3. Glutathione depletion is necessary for ROS formation

Jurkat cells were incubated with FasL (50 ng/ml FasL) for 4 h in the presence or absence of high extracellular GSH medium (25 mM) or NAC (10 mM). Media was switched at the time of FasL stimuli. High glutathione (+GSH) and *N*-acetyl-cysteine (+NAC) medium was made by substitution of NaCl, maintaining the isomolarity of the media. Reactive oxygen species formation was assessed by FACS as explained under "Experimental Procedures" and gated and expressed as in Fig. 2. Plots are representative of at least $n = 3$ independent experiments.

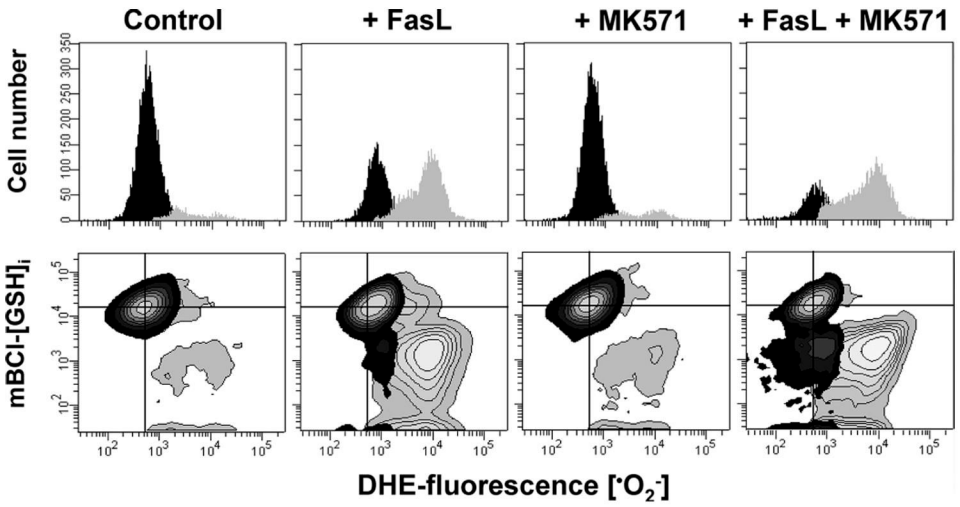

FIGURE 4. Stimulation of GSH depletion enhances ROS formation

Superoxide anion ($^{\bullet}O_2^-$) formation (used as a marker of oxidative stress) and changes in GSH_i were assessed by FACS as in Fig. 1. Apoptosis was induced in Jurkat cells by incubation with FasL (50 ng/ml FasL) for 4 h in the presence or absence of 50 μM MK571. Data are expressed as changes in DHE-fluorescence ($^{\bullet}O_2^-$) represented by frequency histograms (*upper panels*), or in contour plots *versus* changes mBCl fluorescence (GSH_i) (*lower panels*). In contour plots, the quadrant center was set at the mean fluorescence intensity for mBCl and the corresponding ROS dye, as a reference to indicate basal levels of GSH_i and ROS. Populations were gated and represented according to the differences in DHE fluorescence or $^{\bullet}O_2^-$ content, as in Fig. 1*B*. Plots are representative of $n = 3$ independent experiments.

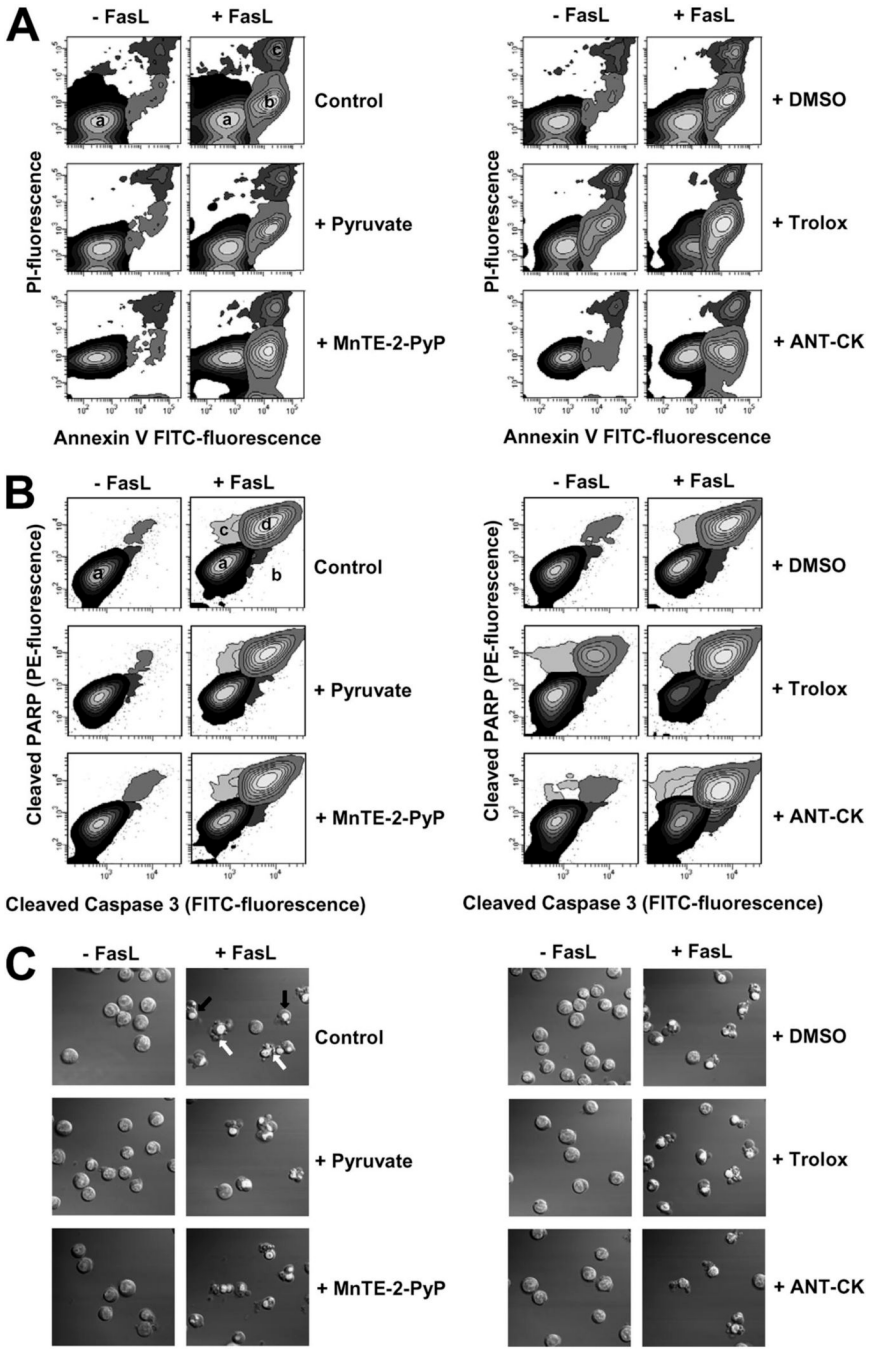

FIGURE 5. Reactive oxygen species do not modulate FasL-induced apoptosis

FasL-induced apoptosis was assessed by (*A*) phosphatidylserine externalization and loss of plasma membrane integrity (cell viability); (*B*) simultaneous detection of cleaved caspase 3 and PARP by FACS; as well as by (*C*) changes in morphological hallmarks of apoptosis which include nuclear condensation, plasma membrane blebbing, and cellular fragmentation. Apoptosis was induced by 50 ng/ml FasL over 4 h. The effect of sodium pyruvate (10 mM), Me_2SO (2%), MnTE-2-PyP (250 μM), trolox (5 mM) was individually assessed or in conjunction (ANT-CK). In *A*, early externalization of phosphatidylserine is shown as an increase in the number of cells that had an increase in annexin V-FITC fluorescence (*population b*), prior to the loss of membrane integrity or high PI fluorescence with respect to control cells (*population*

a). Loss of plasma membrane integrity or cell viability in later stages of apoptosis is reflected as an increase in both PI and FITC fluorescence (*population c*). The contour plots are representative of a single experiment representative of $n = 3$. In *B*, contour plots in control panels show the distribution of cells with background fluorescence for FITC-conjugated anti-cleaved caspase 3, or PE-conjugated anti-cleaved PARP antibodies (*population a, black*). Simultaneous cleavage of caspase 3 and PARP during apoptosis is reflected as a coincident increase in the fluorescence for FITC and PE (*population d, gray*). Other less represented populations indicate cells which are positive for either cleaved caspase 3 (*population b, dark gray*) or cleaved PARP (*population c, light gray*) antibodies respectively, which never reach more than 10% of the total sample. Plots are representative of at least $n = 3$ independent experiments. In *C*, DIC images were obtained to analyze changes in cell morphology during apoptosis. Nuclei condensation is observed as a picnotic and brighter nuclei of cells stained with Hoechst 3342 (see *black arrows* for examples). Examples of cells fragmented or with plasma membrane blebs are pointed by *white arrows*. Images are representative of at least three independent experiments.

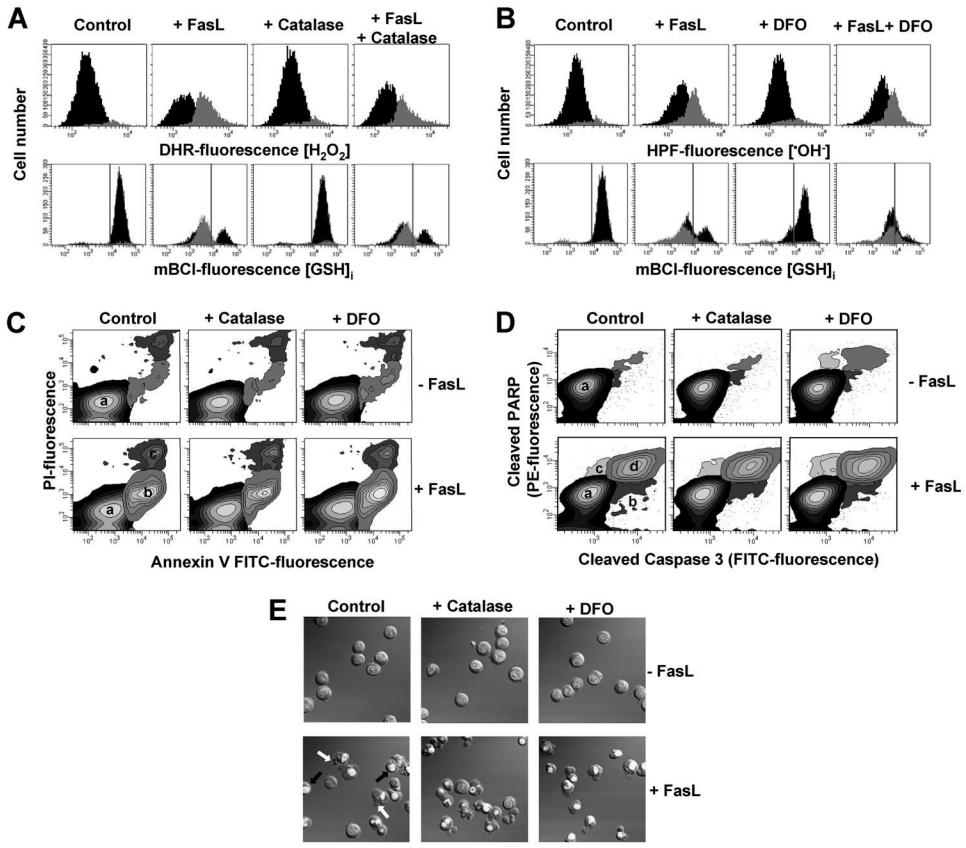

FIGURE 6. Catalase and deferoxamine are ineffective against ROS formation and apoptosis

Apoptosis was induced in Jurkat cells by incubation with FasL (50 ng/ml FasL) for 4 h in the presence or absence of 1000 milliunits/ml catalase (bovine liver) or 1 mM desferoxamine mesylate. Jurkat cells were preincubated in RPMI for 1 h at 37 °C with the agents, and antioxidants remained throughout the experiment. In all cases, control conditions include vehicles at the same concentration. *A* and *B*, simultaneous analysis of changes in GSH content and generation of H_2O_2 or $^{\bullet}OH^{-}$ was performed by FACS. Data are expressed as in Fig. 2. FasL-induced apoptosis was assessed by (*C*) phosphatidylserine externalization and loss plasma membrane integrity; (*D*) simultaneous detection of cleaved caspase 3 and PARP; and (*E*) DIC images depicting nuclear condensation, plasma membrane blebbing, and cellular fragmentation. Results are expressed as in Fig. 5. Plots and images are representative of *n* = three independent experiments.

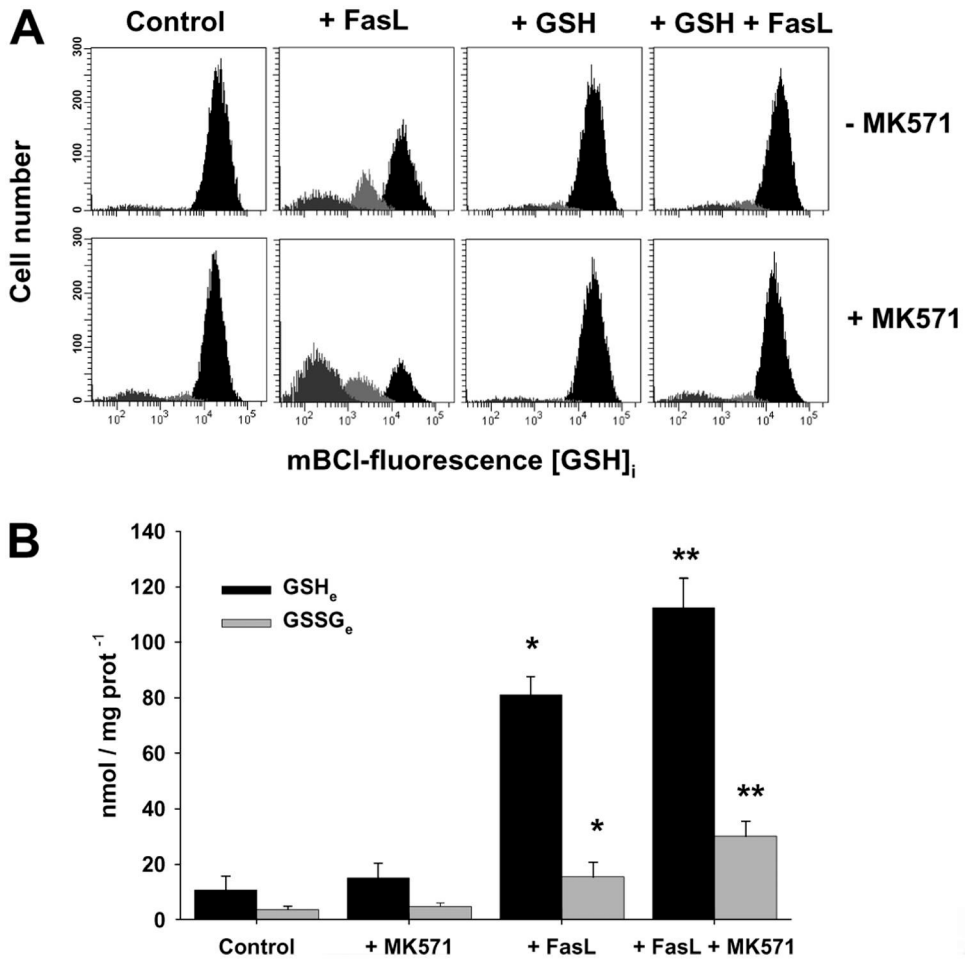

FIGURE 7. Glutathione loss is mediated by a plasma membrane transport, which is stimulated by MK571 and inhibited by high extracellular GSH medium

A, changes in GSH_i were determined by FACS. Effect of 4 h of treatment with 25 ng/ml FasL on the GSH_i of Jurkat cells. Populations were gated according to their GSH_i levels on an mBCl fluorescence *versus* forward scatter plot as explained under "Experimental Procedures." Plots are representative of at least four independent experiments. *B*, extracellular determinations of reduced (GSH) and oxidized (GSSG) glutathione. Cells (2×10^7 cells/ml) were incubated (1 h) with acivicin (250 μM), and then, stimulated with FasL (100 ng/ml) for 2 h with or without MK571 (50 μM). Samples were centrifuged, and aliquots of the media were taken to determine changes in extracellular (*e*) levels of GSH and GSSG. Results are normalized to protein concentration for each sample and are means of $n = 4 \pm$ ES. *, $p < 0.05$, against corresponding control values; **, $p < 0.05$ against corresponding FasL values.

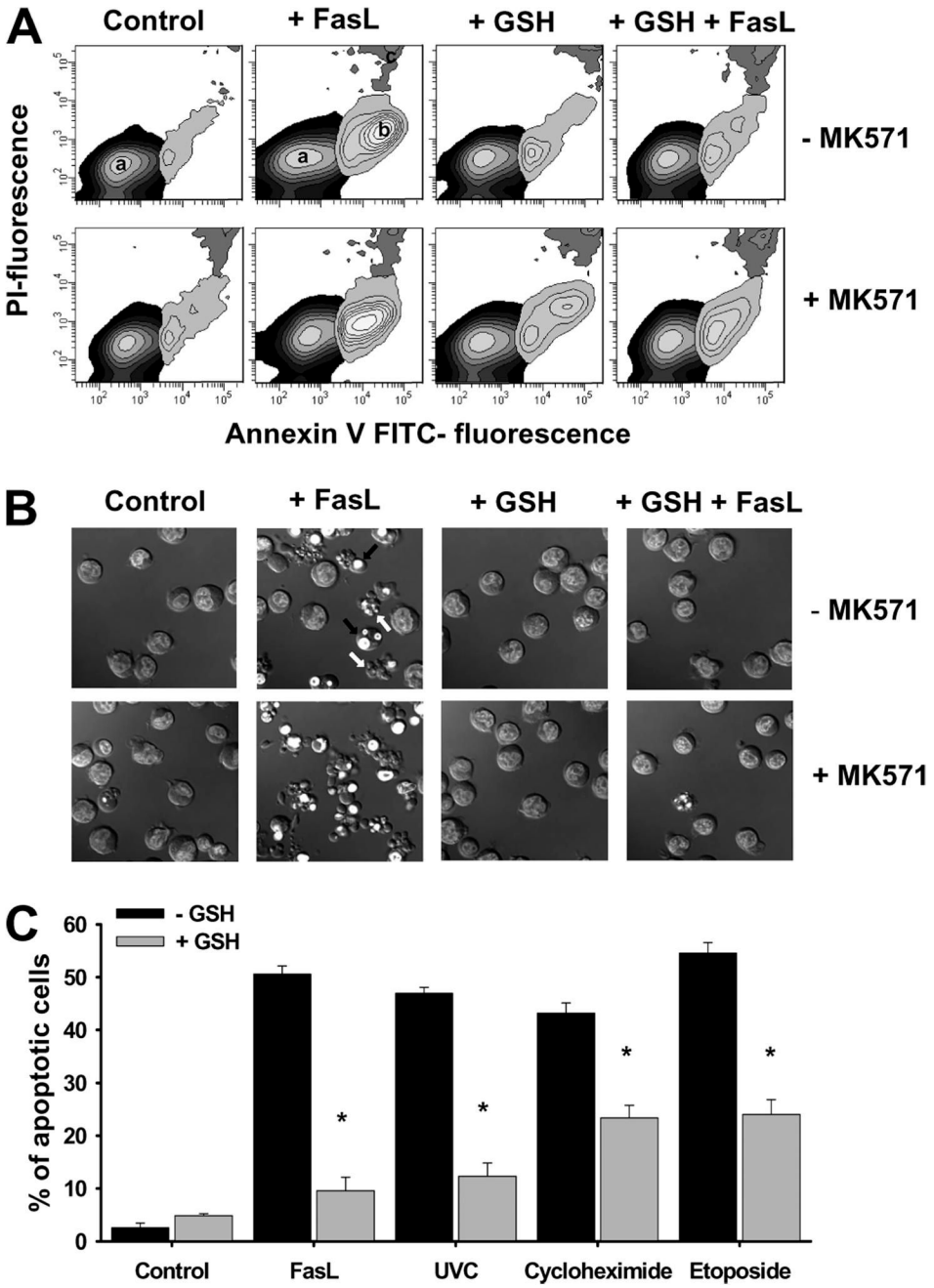

FIGURE 8. Glutathione transport regulates apoptosis induced by distinct stimuli

For the induction of apoptosis, Jurkat cells were incubated with 25 ng/ml FasL for the time indicated. Data are expressed as frequency histograms of mBCl fluorescence. MK571 (50 μM) and high extracellular GSH medium (+*GSH*) were added at the time of FasL stimuli. In *A*, apoptosis was assessed by phosphatidylserine externalization using annexin-FITC staining as explained under "Experimental Procedures." Plots are representative of at least $n = 4$ independent experiments, and in *B*, DIC images were obtained to analyze changes in cell morphology during apoptosis. Images are representative of at least three independent experiments (see Fig. 5). In *C*, the effect of high extracellular GSH on apoptosis induced by 8 h exposure of FasL (25 ng/ml), UVC radiation (15 mJ/cm²), cycloheximide (30 μM), and

etoposide (100 μM) was studied. Apoptosis was assessed by the % of cells with cleaved caspase 3 assessed by FACS as in Fig. 5. Data are expressed as mean ± S.E. of $n = 3$. *, $p < 0.005$ against treatments in the absence of high extracellular GSH (−GSH).

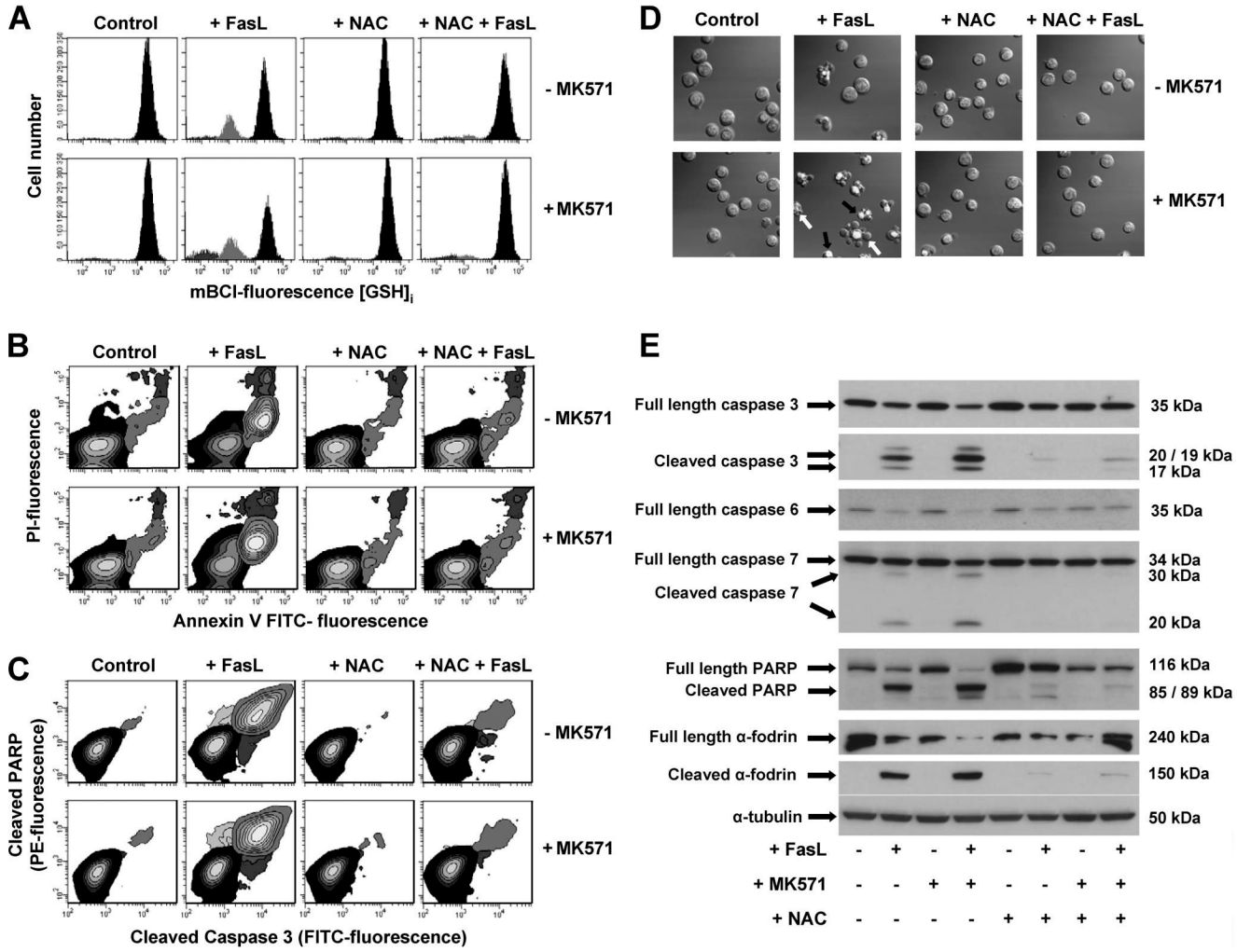

FIGURE 9. ***N*-acetyl-L-cysteine protects against FasL-induced GSH depletion and apoptosis**

Apoptosis was induced in Jurkat cells by incubation with 25 (*A*) and 50 (*B–E*) ng/ml FasL for 4 h. MK571 (50 μM) and high extracellular NAC medium (+NAC) were added at the time of FasL stimuli. *A*, changes in GSH_i were determined by FACS. Populations were gated according to their GSH_i levels on an mBCl fluorescence *versus* forward scatter plot as explained under "Experimental Procedures." FasL-induced apoptosis was assessed by (*B*) phosphatidylserine externalization and loss of plasma membrane integrity; (*C*) simultaneous detection of cleaved caspase 3 and PARP; (*D*) DIC images depicting nuclear condensation, plasma membrane blebbing, and cellular fragmentation; and (*E*) immunoblot detection of full-length and cleaved forms of execution caspases 3, 6, and 7, as well as their substrates PARP and α-fodrin. Results are expressed as in Fig. 5. Plots, images, and blots are representative of $n = 3$ independent experiments.

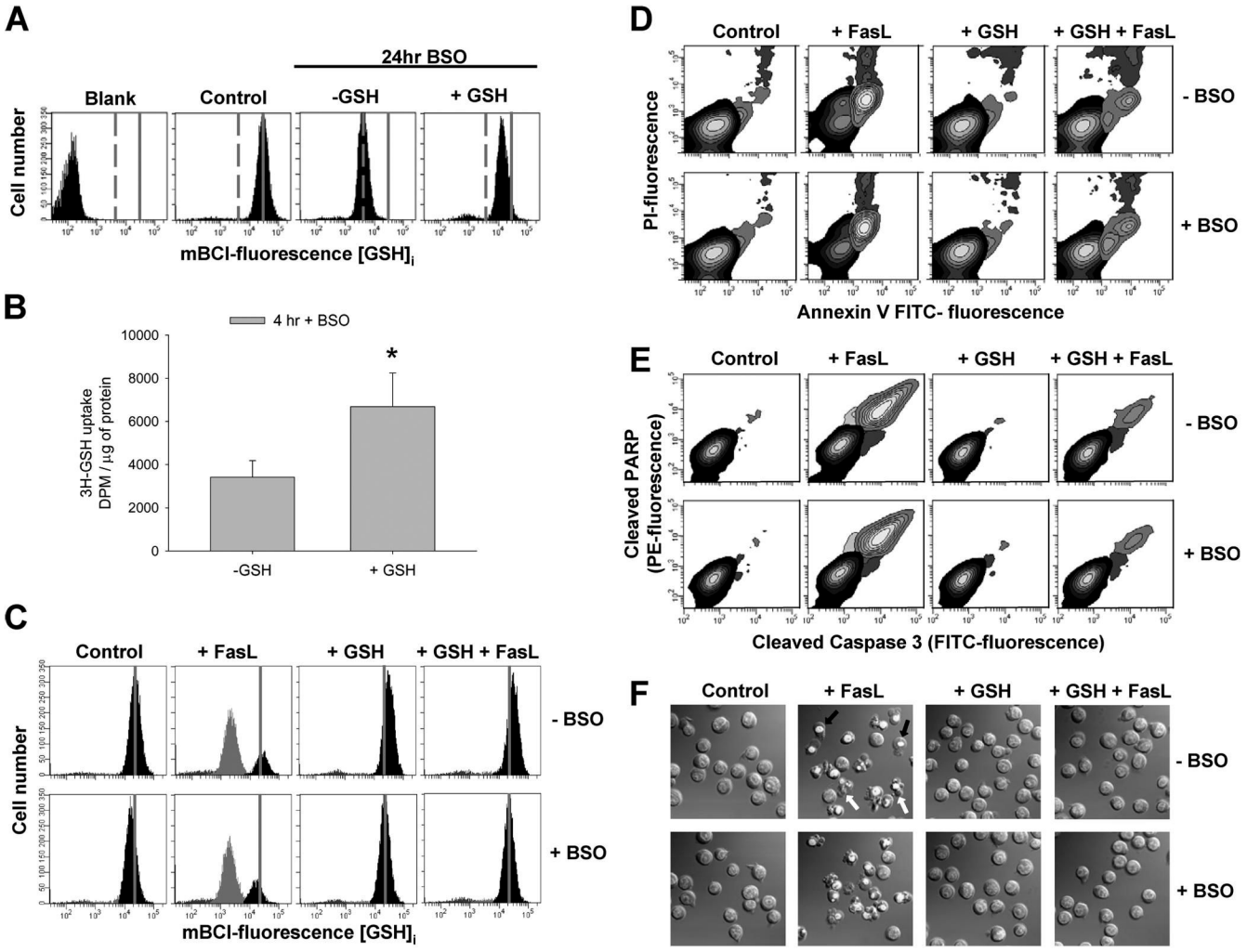

FIGURE 10. High extracellular GSH protects against FasL-induced GSH depletion and apoptosis independent of *de novo* synthesis

The role of *de novo* GSH synthesis in the protective effects of high extracellular GSH was evaluated using BSO (1 mM) an inhibitor of the γGCS. In *A*, cells were treated with BSO for 24 h (−*GSH*). This, significantly depleted cells of GSH_i compared with control cells (*control panel*). When GSH-depleted cells were preincubated for 4 h prior to FACS analysis with high GSH medium (+*GSH*), the GSH_i pool was replenished even in the presence of BSO. In *B*, Jurkat cells were preincubated with 1 μCi of ^{3}H-GSH in the presence of 250 μM acivicin and BSO, with or without of high extracellular GSH. Data are expressed as the amount of radioactivity uptaken by the cells (dpm), normalized by protein concentration per sample. *, $p < 0.05$, against −GSH values. In *C–F*, apoptosis was induced in Jurkat cells by incubation with 50 ng/ml FasL for 4 h. High extracellular GSH medium (+*GSH*) was added at the time of FasL stimuli. *C*, changes in GSH_i were determined by FACS. Populations were gated according to their GSH_i levels on an mBCl fluorescence *versus* forward scatter plot as explained under "Experimental Procedures." After 4 h, BSO starts depleting cells of GSH_i, which is prevented by high extracellular GSH medium. For reference, *grey solid lines* in *A* and *C* depict the medium fluorescence intensity of mBCl in control cells, which reflects basal levels of GSH; *grey dashed lines* in *A* depict the medium fluorescence intensity of mBCl in BSO-treated cells, which reflects depleted levels of intracellular GSH. FasL-induced apoptosis was assessed by (*D*)

phosphatidylserine externalization and loss of plasma membrane integrity; (*E*) simultaneous detection of cleaved caspase 3 and PARP; (*F*) DIC images depicting nuclear condensation, plasma membrane blebbing, and cellular fragmentation. Cells were pretreated with BSO 1 h before the experiment, and it was present throughout the experiment. Results are expressed as in Fig. 5. BSO in *B*–*F* was preincubated for 1 h and was present throughout the experiments. Plots and images are representative of $n = 3$ independent experiments.